MmpL3, the trehalose monomycolate transporter, is stable in solution in several detergents and can be reconstituted into peptidiscs

Kien Lam Ung, Husam Alsarraf, Laurent Kremer, Mickaël Blaise

MmpL3, the trehalose monomycolate transporter, is stable in solution in several detergents and can be reconstituted into peptidiscs.

Kien Lam Ung*[1], Husam Alsarraf *[1,2], Laurent Kremer [1,3] and Mickaël Blaise [#1]

[1]Université de Montpellier, IRIM, CNRS, Montpellier, France.
[2]Department of Molecular Biology and Genetics, University of Aarhus, 8000, Aarhus, Denmark.
[3]INSERM, IRIM, Montpellier, France
* Contributed equally to the work
# Correspondence: mickael.blaise@irim.cnrs.fr

Abstract

Mycobacteria possess a complex and waxy cell wall comprising a large panel of glycolipids. Among these, trehalose monomycolate (TMM) represents abundant and crucial components for the elaboration of the mycomembrane. TMM is synthesized in the cytoplasmic compartment and translocated across the inner membrane by the MmpL3 transporter. Inhibitors impeding TMM transport by targeting MmpL3 show great promises as new antimycobacterials. The recent X-ray or Cryo-EM structures of MmpL3 complexed to TMM or its inhibitors have shed light on the mechanisms of TMM transport and inhibition. So far, purification procedures mainly involved the use of n-Dodecyl-ß-d-Maltopyranoside to solubilize and stabilize MmpL3 from *Mycobacterium smegmatis* (MmpL3Msm) or Lauryl Maltose Neopentyl Glycol for MmpL3 from *Mycobacterium tuberculosis*. Herein, we explored the possibility to solubilize and stabilize MmpL3 with other detergents. We demonstrate that several surfactants from the ionic, non-ionic and zwitterionic classes are prone to solubilize $MmpL3_{Msm}$ expressed in *Escherichia coli*. The capacity of these detergents to stabilize $MmpL3_{Msm}$ was evaluated by size-exclusion chromatography and thermal stability. This study unraveled three new detergents DM, LDAO and sodium deoxycholate that favor solubilization and stabilization of $MmpL3_{Msm}$ in solution. In addition, we report a protocol that allows reconstitution of $MmpL3_{Msm}$ into peptidiscs.

Keywords

Membrane proteins, Mycobacteria, RND transporter, Trehalose monomycolate, MmpL3, Detergents, Peptidiscs

1 Introduction

Mycobacterium tuberculosis (Mtb) and non-tuberculous mycobacteria (NTM) represent a major threat to human health. Current anti-mycobacterial treatments are limited by the rise of multi-, extremely- or totally-drug Mtb resistant strains [1] and by the high intrinsic drug resistance level of some NTM, such as *Mycobacterium abscessus* [2,3], recognized as an emerging human pathogen. There is a clear need to discover new drugs and drug targets to treat these difficult-to-manage bacterial infections. The complex and hydrophobic cell wall of mycobacteria [4] is highly impermeable to drug-like compounds, hence limiting the development of active compounds. On the other hand, since numerous enzymes/pathways and transporters involved in the elaboration of the outer membrane (mycomembrane) are essential and unique to mycobacteria, they represent attractive drug targets. Several studies have shown that the MmpL3 transporter is involved in the assembly of the mycomembrane by exporting giant glycolipids, known as trehalose monomycolate (TMM) that serve as major building blocks of the mycobacterial cell wall [5, 6]. As the transport of TMM appears essential for the survival of mycobacteria, MmpL3 is an essential protein for mycobacterial growth. TMM which is synthesized in the cytoplasm is flipped over the plasma membrane into the periplasmic space by MmpL3, assisted by accessory proteins [7,8], where it is converted to trehalose dimycolate (TDM) by the Antigen 85 complex [9]. TDM, as well as TMM, are inserted into the outer leaflet of the mycomembrane, while mycolic acids from TMM can be attached to arabinogalactan to form the inner leaflet of the mycomembrane.

During the last few years, several effective anti-Mtb and anti-NTM compounds identified from high-throughput drug screenings were proposed to target MmpL3 [5,10–15]. The essential character of this transporter and its propensity to be targeted by various chemical entities support the view that MmpL3 is a highly vulnerable target. Recently, the crystal structure of MmpL3 from *Mycobacterium smegmatis* ($MmpL3_{Msm}$) was reported. The three-dimensional structure of $MmpL3_{Msm}$, lacking its non-essential C-terminus part [16], was solved in its apo form, in complex with several inhibitors [17–19] as well as bound to phosphatidylethanolamine [17]. These structural studies demonstrated that $MmpL3_{Msm}$ belongs to the Resistance-Nodulation-cell Division (RND) superfamily of proteins but remains distant at the sequence and structural level from classical efflux pumps, such as AcrB belonging to the tripartite efflux system [20]. MmpL3 is a monomer harboring two extracellular domains and made of two pseudo symmetrical transmembrane domains, each composed of six transmembrane helices (Fig. 1A). The presence of the C-terminal domain predicted to be flexible and not folded is not conserved in all MmpL3 orthologues and is dispensable for TMM transport [16]. The monomeric state of MmpL3 was further

confirmed by the cryo-electron microscopy (Cryo-EM) structure of MmpL3 from *Mycobacterium tuberculosis* (MmpL3$_{Mtb}$) [21]. A detailed study combining crystal and Cryo-EM structures of MmpL3$_{Msm}$ and including the cryogenic structure of MmpL3$_{Msm}$ bound to TMM has brought important structural elements with respect to the TMM transport mechanism [22].

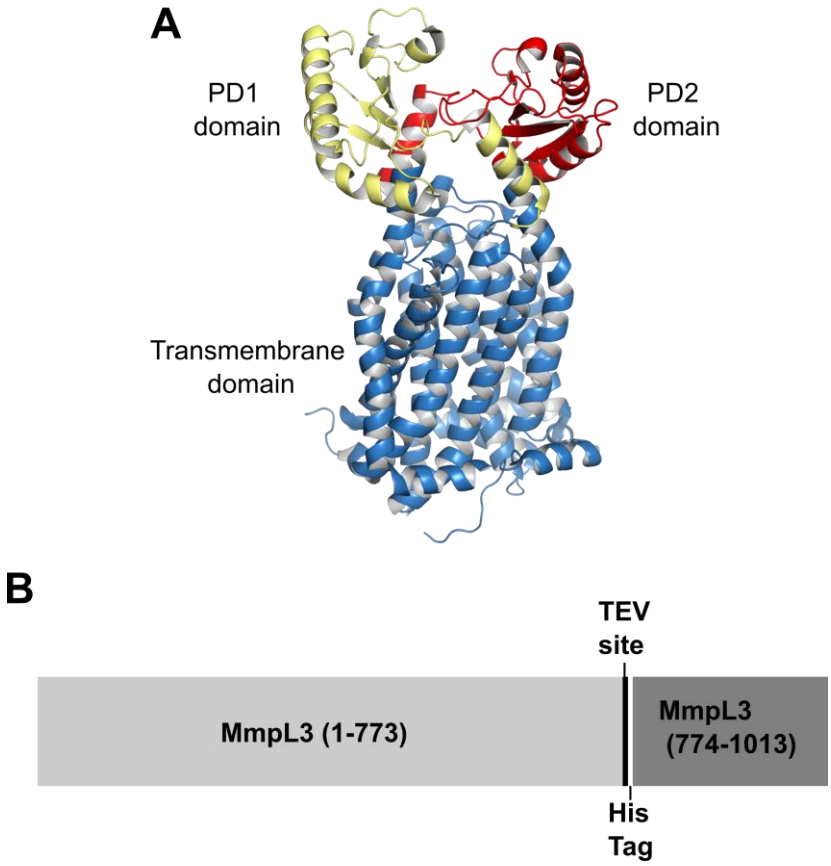

FIGURE1

Figure 1 Overall structure of MmpL3$_{Msm}$ and construct design

A-Representation of the overall crystal structure of MmpL3 from *M. smegmatis* (PDB: 6or2, [17]). The two periplasmic domains PD1 and PD2 are colored in yellow and red, respectively, and the transmembrane part is displayed in blue. **B**- Overview of the construct design used to express MmpL3$_{Msm}$ in this study.

MmpL3 inhibitors bind to the transmembrane domains (TM) of MmpL3 and are likely to block the proton relay and thus the TMM transport [14,18,19,21,23,24]. The mechanism of MmpL3-dependent transport of TMM and the mode of action of the inhibitors are still difficult to apprehend, mainly because of the absence of an in vitro transport assay. While a robust and useful spheroplasts-based assay has been described [14,25], it is not suitable to determine the kinetic parameters of TMM transport mediated by MmpL3.

In the studies describing MmpL3 crystal structures, both *M. smegmatis* [19] and *E. coli* [17] were used to produce recombinant MmpL3. Furthermore, MmpL3 purification

was achieved using n-Dodecyl-ß-d-Maltopyranoside (DDM) for MmpL3$_{Msm}$ and Lauryl Maltose Neopentyl Glycol (LMNG) for MmpL3$_{Mtb}$ [21] as detergents. The present study was undertaken to expand the repertoire of useful detergent(s) to extract, purify and stabilize MmpL3$_{Msm}$, particularly warranted to further decipher the biological/biochemical function of MmpL3 and for subsequent structural investigations. We report here a modified strategy to purify MmpL3$_{Msm}$ using *E. coli* as an expression host, show that MmpL3$_{Msm}$ can be solubilized and stabilized in several detergents and demonstrate the feasibility to insert MmpL3 into peptidiscs. We also evaluate the thermal stability of MmpL3 under these conditions.

2 Materials and methods

2.1 Cloning of MmpL3$_{Msm}$ into pET-15b

The codon-optimized *mmpL3$_{Msm}$* (GenScript) was inserted into pET-15b by sticky-end cloning. Two amplicons corresponding *to mmpL3$_{Msm}$*(1-773) and *mmpL3$_{Msm}$*(774-1013) were amplified by PCR using the following primers and digested with the corresponding restriction enzyme (restriction sites are underlined): Fw_mmpL3Msm(1-773)_NcoI 5′-TTAGTCCATGGGCTTTGCGTGGTGGGGTCGTACC-3′; Rv_mmpL3Msm(1-773)_NheI 5′-ATCCAGCTAGCATGATGATGATGGTGGTGGTGGTGACCCTGGAAGTACAGGTTCTC ACGCTGGTCGGTTTCGCTCTCACGC-3′; Fw_mmpL3Msm(774-1013)_NheI 5′-ATCCAGCTAGCGCGCTGGTTGGTGTGGGTGCGCCGC-3′; Rv_mmpL3Msm(774-1013) BamHI 5′-CTCTAGGATCCTTACAGGCGGCCCTCACGACGCAG-3′. In this design, one extra codon for Gly and one coding sequence for an internal Tobacco Etch Virus (TEV) protease cleavage site (in bold letters), as well as eight histidine codons (in italic letters), and one NheI restriction site were inserted between the Arg773 and Ala774 residues. The two PCR fragments were cloned between the NcoI and BamHI restriction sites in pET-15b, generating pET-15b:*mmpL3$_{Msm}$*. The coding sequence of MmpL3 used in this study corresponds to the UniProt entry: A0QP27. The final construct results in the open reading frame illustrated in Fig. 1B.

2.2 Protein expression, membrane preparation, and protein purification

The recombinant pET-15b:*mmpL3$_{Msm}$* was transformed into the *E. coli* C43(DE3)Δ*acrB* strain [26]. Transformed colonies were used to inoculate a 200 mL pre-culture in Luria-Bertani (LB) media supplemented with 200 μg. mL−1 ampicillin and grown under agitation overnight at 37 °C. This pre-culture was used to initiate a 12 L LB culture in shaker flasks at 37 °C, at 180 rpm and until the OD600nm reached 0.8–1.0. Protein expression was induced with 1 mM of isopropyl-β-D-thiogalactoside (IPTG,

Euromedex) for 3 h at 37 °C. Bacteria were harvested by centrifugation at 6,000g for 20 min, resuspended in buffer A (20 mM Tris-HCl pH 8.0, 0.15 M NaCl, 10% (v/v) glycerol, 0.5 mM β-mercaptoethanol, 1 mM benzamidine) and stored at −20 °C until further use.

Bacteria were thawed in water and treated with 40 mg of lysozyme from the chicken egg for 30 min on ice. From this point, samples were kept at 4 °C for the whole purification process. Cells were opened by sonication (Digital Sonifier, Branson) using the following program: 2 s pulse – 2 s pause, 40% intensity for 3 min and repeated 3 times. Cell lysates were clarified by centrifugation at 28,000g for 1 h. Membrane fractions were pelleted by ultracentrifugation using a 50Ti rotor (Beckman Coulter) at 200, 000 g for 2 h. At this stage, about 1.4 g of membrane per liter of culture were obtained. Two additional membrane washing steps using buffer B (20 mM Tris-HCl pH 8.0, 1 M NaCl, 10% (v/v) glycerol, 0.5 mM β-mercaptoethanol, 1 mM benzamidine) and subsequently buffer A (20 mM Tris-HCl pH 8.0, 0.15 M NaCl, 10% (v/v) glycerol, 0.5 mM β-mercaptoethanol, 1 mM benzamidine) were performed. For each step, the membrane pellet was resuspended by Dounce homogenization and pelleted again by ultracentrifugation and kept on ice overnight.

The next day, the membrane pellet was homogenized in 50 mL of buffer A supplemented with 1% (w/v) of n-Dodecyl-β-D-maltoside (DDM) and stirred for 2 h under gentle magnetic agitation. Insoluble materials were discarded by ultracentrifugation at 200, 000 g, for 1 h at 4 °C, the supernatant was collected, diluted twice in buffer A and gently mixed with Nickel-Nitrilotriacetic acid (Ni-NTA) Sepharose beads (Cytiva) for 30 min prior to loading onto a gravity column. The sample was passed twice and washed with 10 column volumes (CV) of buffer C (20 mM Tris-HCl pH 8.0, 0.15 M NaCl, 10% (v/v) glycerol, 0.5 mM β-mercaptoethanol, 20 mM imidazole, 0.026% (w/v) DDM). Proteins were finally eluted with buffer D (20 mM Tris-HCl pH 8.0, 0.15 M NaCl, 10% (v/v) glycerol, 0.5 mM β-mercaptoethanol, 300 mM imidazole, 0.026% (w/v) DDM). The eluate was mixed with TEV protease (0.025 mg of TEV protease per mg of proteins), dialyzed overnight in buffer E (20 mM Tris-HCl pH 8.0, 0.15 M NaCl, 10% (v/v) glycerol, 0.5 mM β-mercaptoethanol) and centrifuged at 15,000 g for 15 min. The supernatant was applied onto a Ni-NTA Sepharose column to adsorb the His-tagged TEV protease, the cleaved tag, and the uncleaved tagged protein. The flow-through fractions enriched of tag-free MmpL3Msm were then collected and concentrated to 5 mg. mL−1 by ultrafiltration using a 50 kDa cutoff Vivaspin® 20 (Sartorius). A final polishing step was performed using a Superose 6 Increase 10/300 GL column (Cytiva) in buffer F (20 mM Tris-HCl pH 8.0, 0.15 M NaCl, 10% v/v glycerol, 0.026% (w/v) DDM) at a flow-rate of 0.4 mL. min−1. The purest MmpL3Msm fractions, which were assessed by SDS-PAGE stained with Coomassie Blue, were collected and concentrated to 8–10 mg. mL−1 for protein crystallization or subsequent biochemical assays. The protein concentration was determined using a Nanodrop2000c spectrophotometer (Thermo Fisher Scientific). The MmpL3 full-length

construct has a molecular weight of 111 kDa and an extinction coefficient at 280 nm of 103485 M−1cm−1. After TEV cleavage, the truncated MmpL3 version has a molecular weight of 85 kDa and an extinction coefficient of 97985 M−1cm−1, used to determine its concentration.

2.3 Crystallization, data collection, and processing

$MmpL3_{Msm}$ crystals were obtained in hanging drops mixing 2 µL of protein solution at 8 mg. mL−1 with 2 µL of reservoir solution made of 0.1 M ADA and 35% peg 600. Crystals were grown for 3 months at 18 °C and then transferred at room temperature for another 5 months. Crystals were fished with a litholoop without any cryoprotection and cryocooled and stored in liquid nitrogen before data collection. X-ray diffraction data were collected at the PXIII-X06DA beamline at the Swiss Light Source, Villigen, Switzerland. The dataset was recorded on a PILATUS 2M − F detector (Dectris) at a wavelength of 1 Å and a crystal-to-detector distance of 470.0 mm. A total number of 1800 frames were collected with a rotation range of 0.2°. Data were processed with XDS [27]. Crystal anisotropy was assessed on the staraniso server (http://staraniso.globalphasing.org/cgi-bin/staraniso.cgi) (Cambridge, United Kingdom, Global Phasing Ltd). Data collection statistics are listed in Table 2. Molecular replacement was performed with *Phaser* [28] from the *Phenix software* suite [29] and the MmpL3Msm structure [17](PDB, 6or2) was used as a search model. Structure refinement was performed with *phenix.refine* from the *Phenix* software suite [29].

2.4 Detergent solubility screen

The membranes for the detergent solubility screen were prepared, as described in section *2.2* with the exception that the starting volume of culture was 6 L. After ultracentrifugation, the membranes (about 10 g) were resuspended in 10 mL buffer E. The sample was divided into 1 mL aliquots. Proteins were solubilized with the different detergents for 2 h at 4 °C. All the detergents' properties and concentrations used in this study are listed in Table 1. A volume of 200 µL of each sample was then ultracentrifuged for 1.5 h at 200,000 g in a 42.2 Ti Rotor (Beckman Coulter). The non-centrifuged supernatant as well as the ultracentrifuged supernatant were compared and analyzed on 10% SDS-PAGE and revealed with Coomassie Blue and by Western blotting. The detergents' solubility efficiency was assessed by calculating the ratio between the soluble MmpL3 after ultracentrifugation versus before centrifugation. The quantification of the MmpL3 full-length band was determined from the western blot using the Image Lab software version 6.1.0 version from Bio-Rad.

2.5 Detergent screening on size-exclusion chromatography

After the polishing size-exclusion chromatography (SEC) run on Superose® 6 Increase 10/300 GL, $MmpL3_{Msm}$ was concentrated to 2.5 mg. mL−1, using a Vivaspin® 20 with a cut-off of 50 kDa at 4 °C and at 2,700 g. The sample was then centrifuged for 20 min at 4 °C at 16, 200 g, aliquoted in 100 µL, flash-frozen in liquid nitrogen and stored at −80 °C. The aliquots were thawed slowly on ice and then centrifuged for 20 min at 4 °C at 16, 200 g before each SEC run. All the SEC buffers consisted of 20 mM Tris-HCl pH8.0, 150 mM 0.15 M NaCl, 10% (v/:v) glycerol, and three times the critical micellar concentration (CMC) of the respective detergent (Table 1). All detergents were purchased from Anatrace®, except for Tween-20, CHAPSO, and Sodium Deoxycholate (Sigma-Aldrich). All the SEC analyses were performed on a Superose® 6 Increase 10/300 GL column (Cytiva) at a flow rate of 0.4 mL. min−1, at 4 °C, and run on an ÄKTA pure 25 M (Cytiva). Fractions of 0.5 mL were collected.

Table I Detergents properties

Detergent full name	Class	Abbrevi-ation	CMC	Solubilization	SEC Buffer
n-Dodecyl-ß-D-Maltopyranoside	NI	DDM	0.0087%	1%	0.026%
n-Decyl-ß-D-Maltopyranoside	NI	DM	0.087%	1%	0.26%
n-Dodecyl-N,N-Dimethylamine Oxide	Z	LDAO	0.023%	1%	0.069%
n-Octyl-ß-D-Glycopyranoside	NI	OG	0.53%	2%	1.59%
Octaethylene Glycol Monododecyl Ether	NI	C12E8	0.0048%	0.5%	0.014%
Fos-Choline-12	Z	FC12	0.047 %	1%	0.14%
Triton X-100	NI	TX100	0.02%	1%	0.06%
3-([3-Cholamidopropyl]dimethylammonio)-2-hydroxy-1-propanesulfonate	Z	CHAPSO	0.5%	5%	1.5%
Sodium Deoxycholate	I	SD	0.24%	2.4%	0.72%
Tween-20	NI	TW20	0.0072%	1%	0.022%
Sodium Dodecyl Sulfate	I	SDS	0.2%	1%	Not tested

I=ionic, NI=non-ionic, Z=zwitterionic, the CMC values are the ones reported from Anatrace. All the % values are given as w/v.

2.6 Estimation of the apparent molecular weight of MmpL3 by size-exclusion chromatography

The molecular weight of MmpL3 in solution was based on a calibration curve performed on a Superose 6 10/300 GL increase column that has a beads volume of 24 mL. The standard proteins (Sigma-Aldrich) were injected and eluted in 20 mM Tris-HCl pH 8.0, 0.15 M NaCl and 10% glycerol at a flow rate of 0.35 mL. min^{-1}. Thyroglobulin (669 kDa), β-amylase (200 kDa), bovine serum albumin (66 kDa), carbonic anhydrase (29 kDa) and aprotinin (6.5 kDa) eluted at a volume of 13.5, 16.1, 17.1, 18.6 and 20.2 mL, respectively. The void volume of the column was estimated to be 8.2 mL. The apparent mass of MmpL3 was obtained by plotting the partition coefficient Kav against the logarithms of the molecular weight of standard proteins.

2.7 Thermostability assessment of $MmpL3_{Msm}$

$MmpL3_{Msm}$ fraction purified in the different buffers were pooled and concentrated to 0.1 mg. mL−1 using a Vivaspin® 6 concentrator with a cut-off of 10 kDa at 4 °C and at 2,700 g. Samples were then spun down at 16, 200 g for 20 min. For each temperature tested, a 30 µL aliquot was heated for 30 min, followed by cooling on ice for 5 min. Thereafter, the sample was centrifuged for 30 min at 4 °C at 16, 200 g. The supernatant was mixed with 5 µL of 5 x loading dye (310 mM Tris-HCl pH6.8, 10% (w/v) SDS, 10% (v/v) β-mercaptoethanol, 10% (v/v) glycerol and 0.06% (w/v) bromophenol blue). The temperatures tested were ranging from 30 to 90 °C, with a 10 °C increment. The samples were analyzed by 10% SDS-PAGE and the gels were stained with Ready Blue® (Sigma-Aldrich) and destained with dH2O.

2.8 Insertion of $MmpL3_{Msm}$ in NSPr peptidisc

The peptidisc NSPr (Nanodisc Scaffold Peptide) with the following amino acids sequence, Nt-FAEKFKEAVKDYFAKFWDPAAEKLKEAVKDYFAKLWD-Ct [30], was synthesized with a minimum purity of 80% (Genscript). The NSPr solution stock was resuspended in water at 6 mg. mL−1. For reconstitution of the peptidisc complex, 500 µg of MmpL3Msm was mixed with NSPr for 5 min on ice using MmpL3:NSPr molar ratios, ranging from 1:0 to 1:20. The mixtures were then diluted with ice-cold detergent-free buffer (20 mM Tris-HCl pH 8.0, 150 mM 0.15 MNaCl, and 10% (v/v) glycerol) to a final volume of 1 mL. The SEC analysis was performed, as described previously on a Superose® 6 Increase 10/300 GL column. The collected fractions of 0.5 mL and containing $MmpL3_{Msm}$::NSPr, along with pure $MmpL3_{Msm}$ and pure NSPr, as controls, were analyzed on SDS-PAGE, stained with ReadyBlue® (Sigma-Aldrich).

2.9 Assessment of the MmpL3$_{Msm}$::NSPr complex thermostability

The MmpL3$_{Msm}$::NSPr complexes produced using a 1:20 molar M ratio were pooled and concentrated to about 0.2 mg. mL−1. As described above, 30 µL of the sample were heated for 30 min at a temperature ranging from 30 to 90 °C with a 10 °C increment and followed by cooling on ice for 5 min. Samples were then centrifuged at 4 °C and 16, 200 g for 30 min, mixed with 5 µL loading dye and analyzed by 10% SDS-PAGE.

2.10 Western blotting

Proteins were separated by SDS-PAGE and transferred onto a nitrocellulose membrane by electrophoresis applying a current of 300 mA for 45 min in ice-cold transfer buffer (20% ethanol, 20 mM Tris, 150 m0.15 M glycine, pH 9.0) using a Mini Trans-Blot Electrophoretic Transfer Cell (Bio-Rad). After the transfer, the nitrocellulose membrane was blocked for 1 h at 4 °C with blocking buffer (1x Phosphate Buffered Saline (PBS), 0.2% Tween-20 and 5% w/v skimmed milk powder), followed by overnight incubation with monoclonal anti-His-tag primary antibodies (Sigma-Aldrich) diluted 5000 times in blocking buffer. Membranes were then washed twice with wash buffer (1x PBS buffer supplemented with 0.2% Tween-20) for 20 min at 4 °C and incubated for 3 h with an anti-mouse antibody conjugated to horseradish peroxidase diluted 10 000 times (Sigma-Aldrich). Membranes were washed once with wash buffer and twice with 1xPBS and revealed using the SuperSignal West Pico Plus Chemiluminescent Substrate (ThermoScientific) on a ChemiDoc™ Gel Imaging System (Bio-Rad).

3 Results

3.1 Overexpression of MmpL3$_{Msm}$ in *E. coli*

A synthetic gene construct with optimized codons for E. coli expression was synthesized and cloned into pET-15b. The construct was designed so that the first 773 amino acids (truncated MmpL3) were followed by a TEV cleavage site and an octahistidine-tag (Fig. 1B). The polyhistidine-tag was cloned in frame with the sequence coding the C-terminal domain (residues 774–1013) of MmpL3$_{Msm}$. The theoretical molecular weight of this chimeric protein is 111 kDa. We assessed the expression level of this protein in E. coli C43(DE3)ΔacrB by inducing expression with 1 mM IPTG for 3 h at 37 °C or overnight at either 37 °C or 18 °C. Western blot analysis attests to the presence of the protein in the crude extracts under the 3 conditions. Higher levels of the soluble form of the protein (MmpL3$_{Msm}$-FL) were achieved during overnight growth at 37 °C (Fig. 2A). However, since more proteolysis was observed during purification when the expression was performed overnight at 37 °C or 18 °C (not shown), all subsequent experiments were conducted after induction with IPTG for 3 h at 37 °C. We assume that degradation

occurred at the C-terminus as it was previously reported that this part of MmpL3 is disordered and unstable [17,22] which was further confirmed with large scale purification.

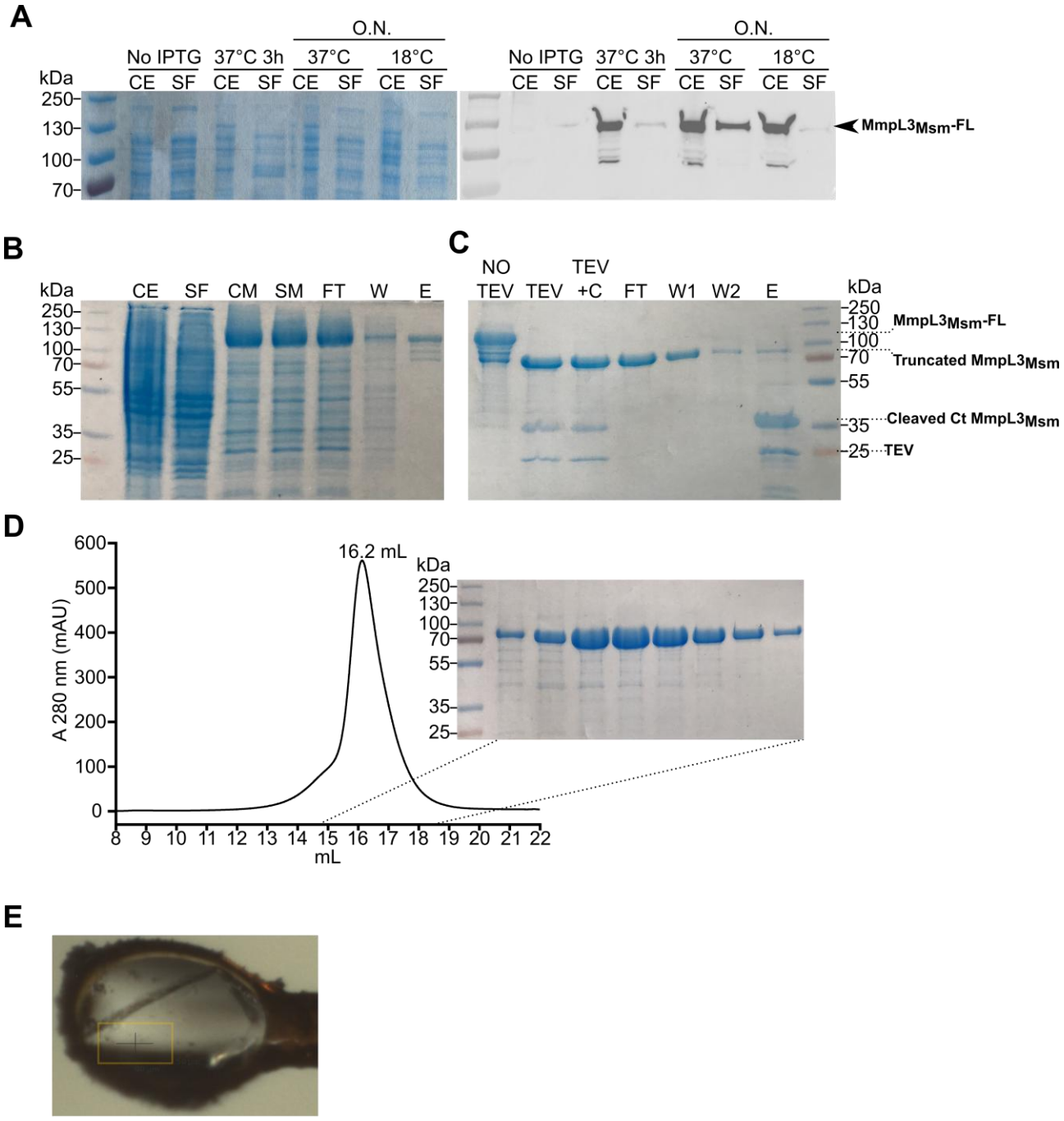

FIGURE 2

Figure 2 Expression test and large-scale purification and crystallization of MmpL3$_{Msm}$ in DDM.

A-Expression tests of MmpL3$_{Msm}$ were performed in *E. coli* C43Δ*acrB* strain under three different conditions. The left panel corresponds to the Coomassie-stained SDS-PAGE. The negative control was performed at 37 °C for 3 h without IPTG. Three different conditions were tested to induce protein expression with 1 mM IPTG at 37 °C for 3 h and overnight at 37 °C or 18 °C. The right panel shows the Western blot corresponding to the same samples. Bands were revealed using primary antibodies directed against the poly-histidine-tag. CE (crude extract) corresponds to the sample after bacterial lysis obtained by sonication

while SF (soluble fraction) is the lyzed fractions after centrifugation, containing the soluble proteins. **B**-Purification of MmpL3$_{Msm}$ on immobilized metal affinity chromatography (IMAC). CE crude extract; SF, soluble fraction; CM crude membranes; SM soluble membranes; FT Flow-through; W wash; E elution. **C**-Second step of IMAC purification after cleavage of the C-terminal end and the poly-histidine tag. NO TEV corresponds to the same sample as the elution fraction (E) of the 1st IMAC. TEV corresponds to the sample that has been dialyzed overnight in the presence of the TEV protease. TEV + C indicates that it is the TEV sample that was centrifuged and represents the second IMAC column load. The cleavage is efficient as the protein molecular weight in NO TEV sample is shifting from 111 kDa to 85 kDa in the TEV-treated condition. FT corresponds to the Flow-through; W1 and W2 stand for wash 1 and wash 2 and E is the column elution. MmpL3$_{Msm}$ lacking its tag and C-terminal end is mainly eluted in the FT and to a lower extent in the wash fractions. The elution fractions contain mainly the cleaved C-terminus tag, the TEV protease and small fractions of the uncut MmpL3$_{Msm}$. **D**-Elution profile of truncated MmpL3$_{Msm}$ on size-exclusion chromatography. 5 mg of protein were loaded on the 24 mL Superose® 6 Increase 10/300 GL column and eluted at a flow rate of 0.4 mL. min−1. Fractions of 0.5 mL were collected. The peak and side fractions were analyzed on Coomassie Blue-stained SDS-PAGE. **E**-Crystallization of MmpL3$_{Msm}$. Picture of the best diffracting MmpL3$_{Msm}$ crystal under a cryostream at the Swiss Light Source PXIII beamline and obtained in sitting drop and fished in a litholoop. The size of the crystal is about 180x80x10 μm.

3.2 Large scale purification of MmpL3$_{Msm}$ in DDM

To assess whether the chimeric MmpL3$_{Msm}$ protein can be obtained in good yields, large-scale expression and purification were done. DDM was chosen to solubilize MmpL3Msm from the membranes and maintained in all subsequent purification steps on immobilized metal affinity chromatography (IMAC) and size-exclusion chromatography (SEC). DDM was tested first because it was previously described as a good detergent to extract MmpL3 from E. coli or mycobacterial membranes [17,19,25].

MmpL3$_{Msm}$ was extracted from the membrane with 1% (w/v) DDM and purified following three consecutive chromatography steps while maintaining DDM at three times the critical micelle concentration (CMC) (0.026%; w/v). After elution from the IMAC, three major bands, attributed to proteolysis, could be seen below the full-length MmpL3$_{Msm}$ (Fig. 2B). After elution, the tag and the C-terminal part of MmpL3$_{Msm}$ were cleaved using the TEV protease during the dialysis step. The tag cleavage is very efficient as most of the protein was lacking the C-terminal domain, resulting in a molecular weight shift from 111 kDa to 85 kDa (Fig. 2C). The TEV cleaved protein was loaded again on IMAC enabling it to bind the cleaved C-terminal domain and the tags as well as the TEV protease that also possess a poly-histidine-tag (Fig. 2C). The protein degradation observed after the first IMAC could not be seen after the second IMAC and TEV cleavage, suggesting that degradation occurs at the C-terminal part of MmpL3$_{Msm}$ (Fig. 2C).

The cleaved MmpL3$_{Msm}$ collected in the flow-through of the 2nd IMAC step was then concentrated to 5 mg. mL−1 and loaded onto a SEC column. This final step on Superose 6 column led to MmpL3$_{Msm}$ sample that appears monodisperse, as shown by the

homogeneous peak on SEC (Fig. 2D). The protein is very pure after these three purification steps as judged by SDS-PAGE and Coomassie-blue staining. Overall, this multi-step procedure yielded 0.4 mg of pure MmpL3$_{Msm}$ per liter of culture.

3.3 MmpL3$_{Msm}$ crystallization

We next assessed the quality of the purified MmpL3$_{Msm}$. As mentioned earlier, monitoring the MmpL3$_{Msm}$ activity remains so far impossible due to the lack of an in vitro TMM transport assay. As an alternative, we tested the capacity of MmpL3$_{Msm}$ to crystallize, since the capacity of a membrane protein to crystallize is often correlated to high protein quality [31]. MmpL3$_{Msm}$ crystals could be obtained in several conditions and the best dataset showed that resolution extended to 4.2 Å and that the protein crystallized in a new crystal form (Fig. 2E and Table 2). To confirm that MmpL3$_{Msm}$ was the entity that crystallized (rather than a possible contaminant), we solved the structure by molecular replacement using *Phaser* [28] from the *Phenix software suite* [29] and the MmpL3$_{Msm}$ structure (PDB 6or2) as a search model [17]. Two molecules of MmpL3$_{Msm}$ were found in the asymmetric unit, thus validating the nature of the crystals. To further validate the molecular replacement solution, we performed one round of refinement that includes bulk solvent correction, the initial R/R$_{free}$ values 0.52/0.55 drop to 0.37/0.42 strongly suggestive of the correct molecular replacement solution. However, the electron density was of insufficient quality to further exploit the structure. The crystal's anisotropy might be one of the reasons for the low electron density map quality (Table 2). Despite these crystallographic pitfalls, these experiments strongly attest that our construct design and purification strategy can lead to high protein quality.

Table II: Data collection statistics

Beamline	SLS-PXIII-X06DA
Wavelength (Å)	1
Space group	$P2_1$
Unit cell (Å,°)	73.43 231.81 81.48 90.0 109.87 90.0
Low-resolution limit (Å)	48.85
High-resolution limit(Å)	4.19 (4.41-4.19)
Rmeas	0.143 (0.91)
Total number of observations	62486 (2904)
Total number of unique Observations	9371 (469)

Mean(I)/σ(I)	8.4 (2.5)
Completeness %, spherical	50.1 (18)
Completeness %, ellipsoidal	88.4 (97.6)
Multiplicity	6.7 (6.2)
CC(1/2)	0.99 (0.69)

3.4 Detergent screen solubility

Our study aimed also at assessing whether MmpL3$_{Msm}$ can be extracted from *E. coli* membranes with other surfactants than DDM. To do so, nine additional detergents were tested for their capacity to solubilize MmpL3$_{Msm}$. We have tried three zwitterionic detergents (FC12, LDAO and CHAPSO), six non-ionic detergents (DM, DDM, OG, C12E8, TX100 and TW20) and finally one ionic detergent (SD) and also SDS that served as a positive control. The detergent choice was driven by the fact that we wanted to cover different classes and types of detergents and also because these detergents are some of the most widely used in biochemical and structural studies [32]. All detergents were tested at the final concentrations listed in Table 1. After incubation of the membranes with the detergents, one ultracentrifugation step was performed. The non-centrifuged and centrifuged samples were then compared by SDS-PAGE and Western blotting using an anti-his tag primary antibody. The efficacy of solubilization was defined as described in section *2.4*.

Several detergents were suitable for extraction and solubilization of MmpL3$_{Msm}$ as judged by the presence of the protein in the supernatant after ultracentrifugation (Fig. 3). TX100, C12E8, DM, DDM, LDAO were able to solubilize over 75% of MmpL3 with an efficiency close to the positive control SDS. SD and CHAPSO were also quite efficient with a solubilization efficacy of about 60%. Only a very small protein fraction was lost after the ultracentrifugation step with these surfactants (Fig. 3). OG and TW20 seemed also suitable for the extraction though to a lower extent as a significant proportion of the protein precipitated after centrifugation as only about 30% and 10% of the protein was solubilized with these two detergents, respectively (Fig. 3).

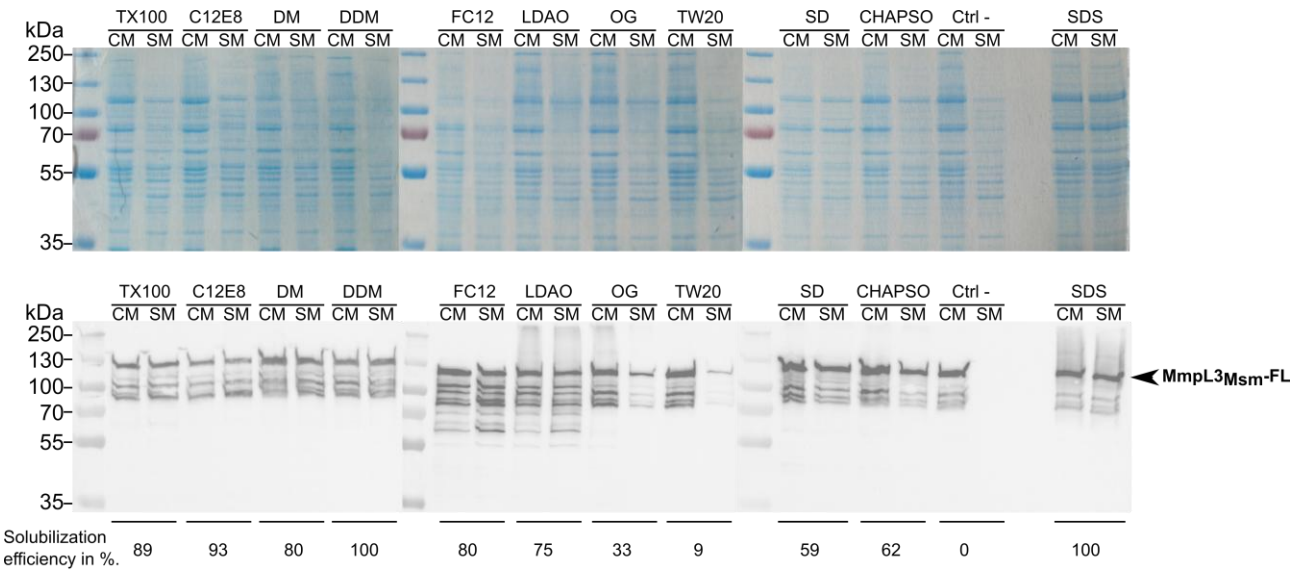

FIGURE 3

Figure 3 Detergents screening for optimal MmpL3$_{Msm}$ solubilization

The upper panels correspond to the Coomassie Blue-stained SDS-PAGE of the different samples while lower panels are the corresponding Western blots, revealed using primary anti-histidine tag antibodies. CM (crude membranes) corresponds to the resuspended membranes incubated with or without detergents. SM (soluble membranes) corresponds to the membrane fractions obtained after ultracentrifugation and represents membrane proteins that have been successfully solubilized. Bands corresponding to the MmpL3$_{Msm}$ full-length protein (MmpL3$_{Msm}$-FL) are indicated by the arrow. Control negative (Ctrl -) has been treated under similar conditions but without any detergent. The bands located below MmpL3$_{Msm}$-FL are attributed to proteolysis occurring at the C-terminus of the protein. The percentage of solubilization efficiency is indicated below each detergent and determined as described in section *2.4*

3.5 Stability of MmpL3$_{Msm}$ in detergents

The detergent solubilization screen suggested that several surfactants could efficiently extract MmpL3$_{Msm}$ from *E. coli* membranes. However, this does not necessarily indicate that MmpL3$_{Msm}$ is kept in a stable and homogenous form in solution with these detergents, particularly at concentrations below the CMC. SEC was performed using the ten different detergents to address the stability of MmpL3$_{Msm}$ in solution. The protein was first purified in DDM and then the detergent exchange was performed using SEC. All SEC elution buffers contained detergent concentrations corresponding to three times their CMC.

In DDM, the detergent of reference, MmpL3$_{Msm}$ is eluted as a homogenous peak and is eluted at 16 mL (Fig. 4). MmpL3$_{Msm}$ behaved similarly in DM. The elution profiles of MmpL3$_{Msm}$ in DDM and DM were homogeneous and characterized by a smaller peak before the main one. LDAO seemed also appropriate, with a very homogenous and sharp peak. MmpL3$_{Msm}$ was also eluted as sharp peaks in the presence of SD and CHAPSO. All

the remaining detergents tested (OG, C12E8, TW20, FC12 and TX100) were less favorable, albeit none of them led to highly aggregated proteins since no protein was observed in the void volume of the column estimated to 8.2 mL. Nonetheless, the elution peaks with these detergents are not as sharp and the elution volumes are lower than 15.5 mL, perhaps indicating the formation of higher oligomers and/or protein aggregation. We indeed estimated from the column elution volume (Fig. 4) that in DDM, DM, SD and CHAPSO, that MmpL3 has an apparent molecular weight ranging from 116 kDa to 173 kDa, is suggestive a of monomer (considering the contribution of the detergent and/or lipids corona/belt surrounding the protein), while in all the other detergents the apparent mass is increasing with a maximum of 382 kDa for TW20.

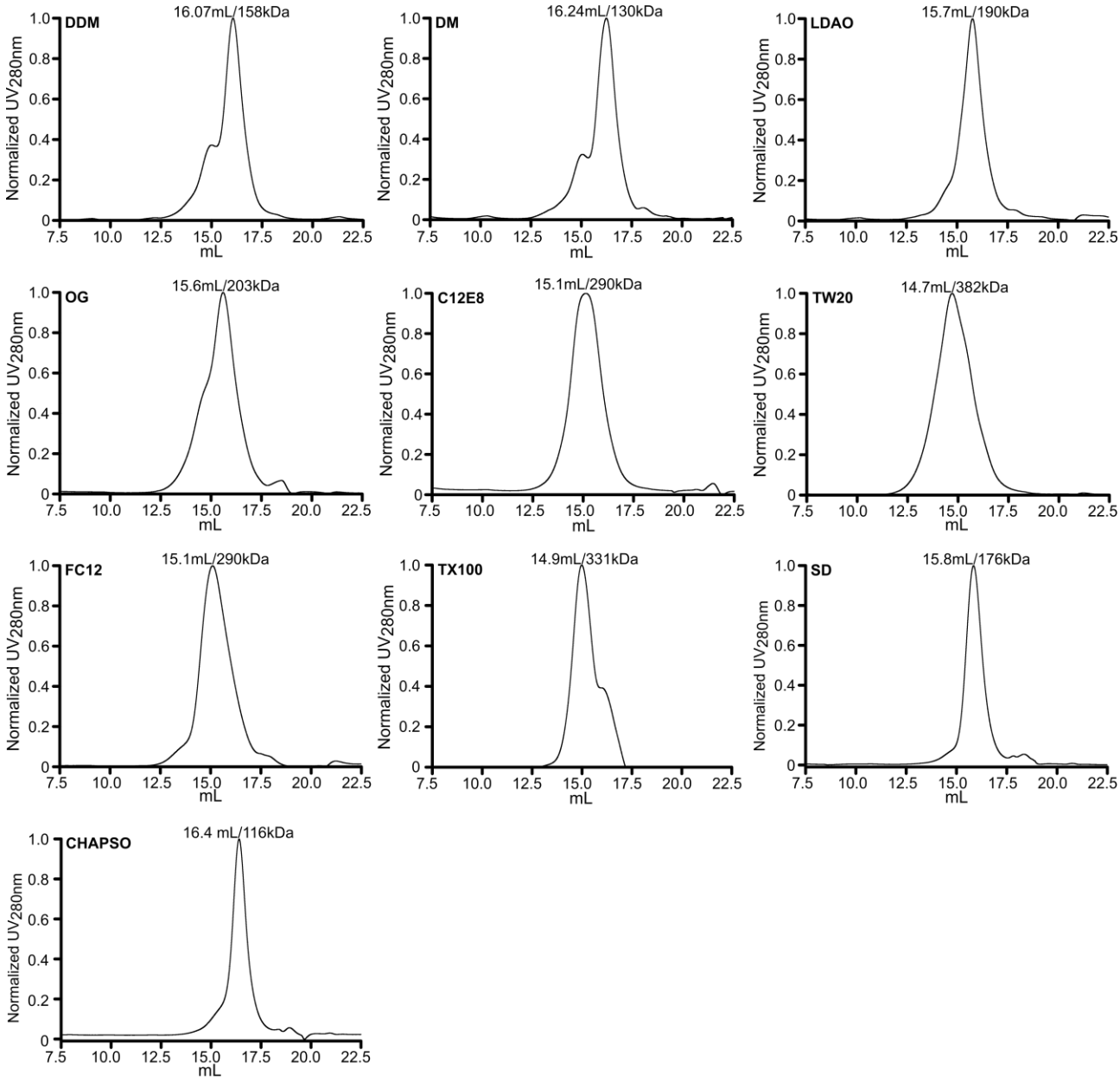

FIGURE 4

Figure 4 Stability of MmpL3$_{Msm}$ in solution

The chromatograms display the elution profiles of MmpL3$_{Msm}$ on a Superose® 6 Increase 10/300 GL column. All the runs were performed under similar conditions: 250 μg of the sample were injected and eluted at a flow rate of 0.4 mL. min−1 and 0.5 mL fractions were collected. The absorbance at 280 nm has been normalized with Graphpad Prism so that the highest value for each run corresponds to 1. All the elution volumes are indicated in mL above each peak. Of note, for TX100 an absorbance peak displayed negative values due to the nature of TX100, starting from 17.5 mL to 22.5 mL, and therefore this part of the graph was excluded for presentation purposes. The estimated molecular weight (in kDa) is indicated above each peak and was calculated thanks to the comparison with known molecular weight markers, as indicated in section *2.6*.

3.6 Stability of MmpL3$_{Msm}$ into peptidisc

In recent years, alternatives to detergents were employed for biochemical or structural purposes. This includes the use of polymers such as amphipols [33], Styrene maleic acid lipid particles (SMALPs) [34] or the use of peptides that enable to trap the membrane protein into nanoparticles through the use of nanodiscs [35] or saposin-lipoparticles [36]. The use of nanodiscs to embed MmpL3$_{Msm}$ has been particularly successful to generate a high-resolution Cryo-EM structure of MmpL3 bound to TMM [22]. Another recently developed technology allows the embedding of membrane proteins into the form of nanoparticle-like structures without the need to add extra lipids, in contrast to nanodiscs or salipro. This technique uses multiple copies of an amphipathic bi-helical peptide, named peptidisc or Nanodisc Scaffold Peptide (hereafter termed NSPr), displacing the detergent and wrapping the protein [30]. We thus assessed whether MmpL3$_{Msm}$ could be entrapped into NSPr. The protein was first purified as described in section *3.2* using DDM and MmpL3$_{Msm}$ was then incubated with NSPr for a few min, loaded onto a SEC column and eluted in a detergent-free buffer. Various MmpL3$_{Msm}$:NSPr molar ratios were tested (ranging from 1:0 to 1:20) to identify optimal conditions allowing to embed the majority of MmpL3$_{Msm}$ (Fig. 5A). MmpL3$_{Msm}$:NSPr ratios from 1:1 till 1:5, and to a lesser extend 1:10 led to protein aggregation (Fig. 5A). The 1:20 was the optimal MmpL3$_{Msm}$:NSPr ratio to enable reconstitution of MmpL3Msm into peptidiscs to obtain stabilization of MmpL3$_{Msm}$ as seen on SEC with an elution peak at 16.7 mL. This corresponds to an apparent molecular weight of 94 kDa and is likely to be monomeric MmpL3. The presence in the same fractions of both MmpL3$_{Msm}$ and NSPr was also confirmed by SDS-PAGE (Fig. 5B).

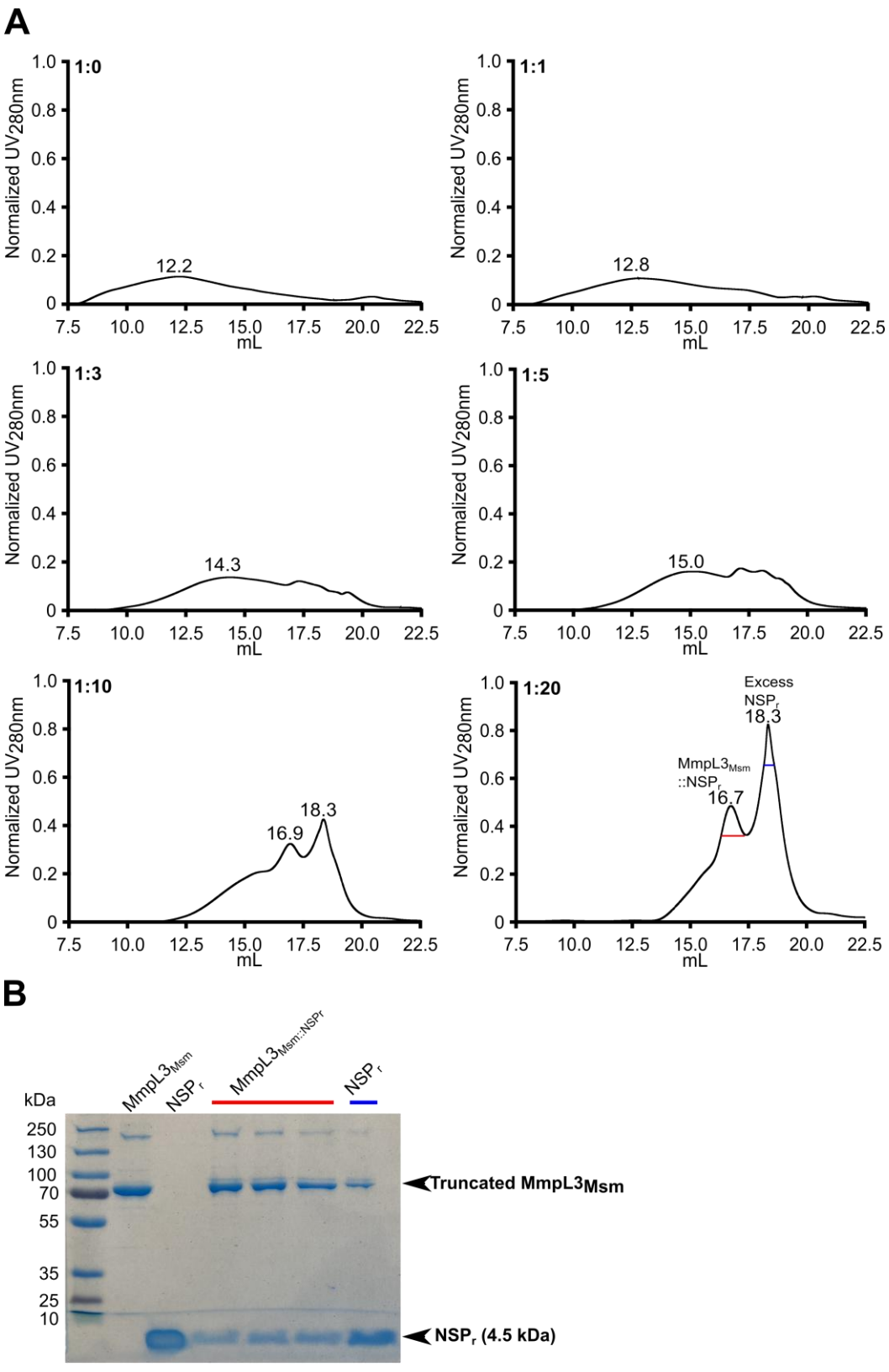

FIGURE 5

Figure 5 Reconstitution of MmpL3$_{Msm}$ into peptidiscs

A-The chromatograms display the elution profiles of the truncated MmpL3$_{Msm}$ on a Superose® 6 Increase 10/300 GL column. The absorbance at 280 nm has been normalized with Graphpad Prism so that the highest

value for each run corresponds to 1. Elution volumes are indicated (in mL) above each peak. The MmpL3$_{Msm}$:NSPr molar ratios are indicated in the upper left section of each chromatogram. A negative control (ratio 1:0) consisting of injecting MmpL3$_{Msm}$ without pre-incubation with NSPr attests to the high aggregation properties of the protein. **B**- The Coomassie Blue-stained SDS-PAGE confirms the presence of MmpL3$_{Msm}$ and NSPr found in the 16.7 mL elution peak and a large excess of NSPr found in the elution peak at 18.3 mL. Pure MmpL3$_{Msm}$ and pure NSPr were loaded as controls.

3.7 Thermal stability of MmpL3$_{Msm}$

Further assessments on the stability of MmpL3$_{Msm}$ in different detergents and peptidisc environments were done by measuring the thermal stability of the various preparations. MmpL3$_{Msm}$ was heated for 30 min from 30 °C to 90 °C, spun down and the supernatant loaded on SDS-PAGE followed by Coomassie Blue staining. Of note, the denatured protein did not always precipitate after centrifugation but thermal denaturation was often correlated with the appearance of large protein aggregates on SDS-PAGE (Fig. 6). In DDM, DM, and SD, MmpL3$_{Msm}$ starts to denature around 50 °C. LDAO and peptidisc seem also rather good to stabilize the protein but to a lower extent as compared with the above-cited detergent as more aggregated protein could be seen at 50 °C (Fig. 6). In OG, C12E8, TX100, CHAPSO, and TW20, thermal denaturation occurs at lower temperatures and large aggregates are even present for OG at 4 °C. TX100 does not appear as a good stabilizer as large aggregates are detected at low temperatures and, at temperatures >60 °C, aggregates were so pronounced that the protein failed to migrate into the gel. These results indicate that OG and TX100 are not suitable to stabilize MmpL3$_{Msm}$. Concerning FC12, even at 90 °C very few amounts of proteins seemed to precipitate or form aggregates in the gel. The harsh zwitterionic detergent properties of FC12 may explain this behavior of the protein after denaturation on SDS-PAGE. This assay also confirms the stability of MmpL3Msm when inserted into peptidisc nanoparticles, with a thermal denaturation profile very similar to the ones of DDM, DM, or LDAO profiles.

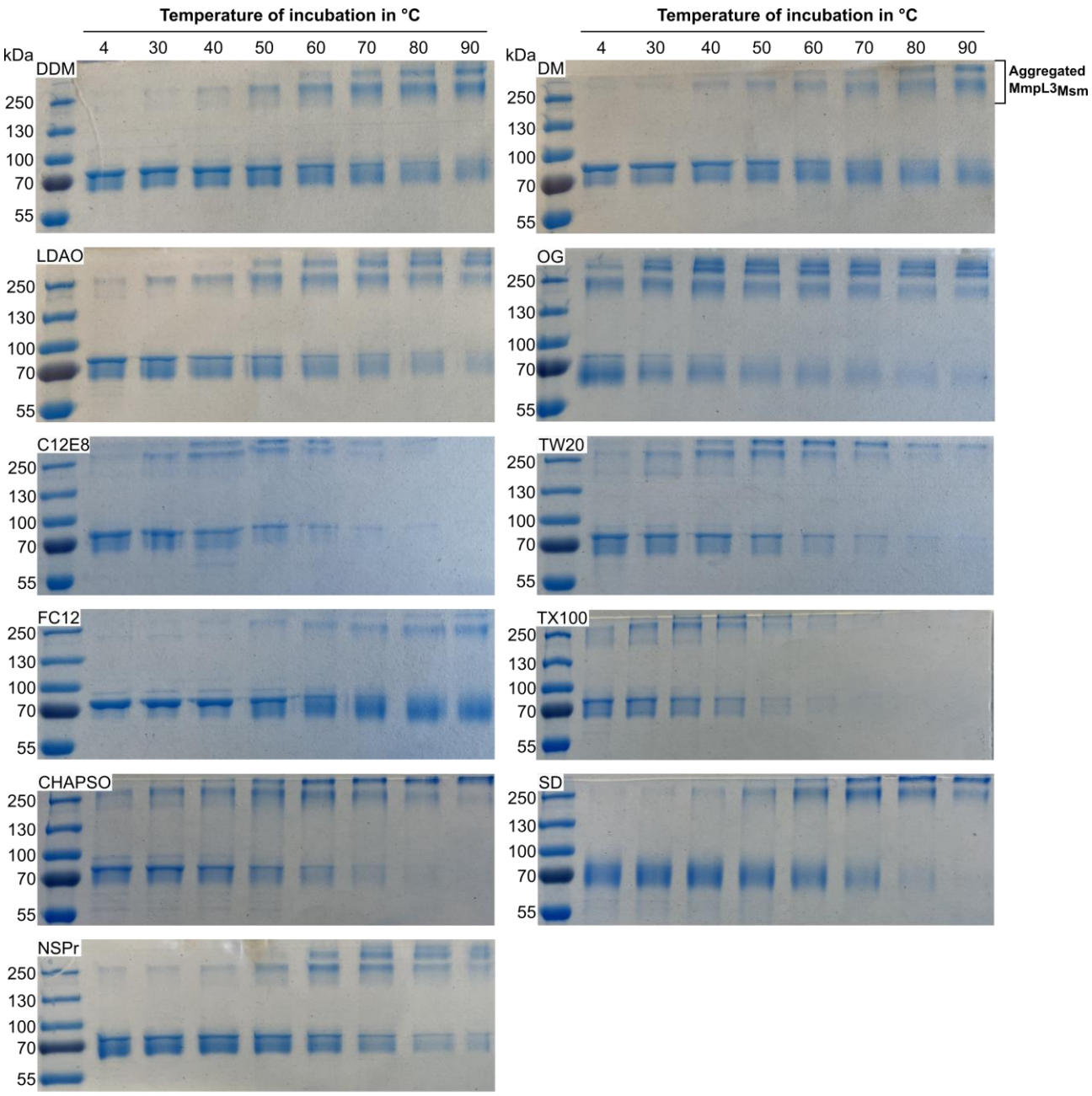

FIGURE 6

Figure 6 Thermal stability of MmpL3$_{Msm}$ in the different types of detergent and reconstituted in peptidiscs

The appearance of large protein aggregates in the gel or the absence of MmpL3Msm band were considered as signs of protein denaturation. Protein aggregation resulted in the form of multiple bands (aggregated MmpL3Msm) migrating over the 250 kDa molecular weight marker and correlated with the disappearance of the stable MmpL3Msm band at 85 kDa

4 Discussion

A surprisingly large variety of recent chemical scaffolds against *M. tuberculosis* or NTMs has been assigned to target MmpL3 activity, leading to the view that this transporter could represent the Achilles' heel of mycobacteria [5,11,37]. This has emphasized the need for a better functional and structural characterization of MmpL3$_{Msm}$. In this study, we explored the possibility to develop new ways to solubilize MmpL3$_{Msm}$ from *E. coli* membrane and assessed the stability of the protein in solution in various detergents by SEC and thermal denaturation. Among the ten detergents tested (including the reference DDM previously used in structural and biochemical studies [17,19,25]), we identified seven detergents (TX100, C12E8, DDM, DM, FC12, SD, and CHAPSO) that could very efficiently solubilize the protein. Three other surfactants (LDAO, OG, and TW20) were prone to solubilize MmpL3$_{Msm}$ but with a lower efficacy. Since the ionic (SD), non-ionic (TX100, DDM, DM, C12E8), or zwitterionic (CHAPSO, FC12) detergents share the same efficacy of solubilization, it can be inferred that the class of detergent is not correlating with the efficacy of solubilization. In addition, the solubilization efficacy does neither seem to correlate with the CMC (CHAPSO with a high CMC (0.5%) is as prone to solubilize MmpL3Msm as DDM that has a low CMC) nor with the length of the alkyl chain.

Importantly, none of the detergents tested led to high aggregative forms of MmpL3$_{Msm}$ on SEC. While DDM, DM, LDAO, SD, CHAPSO and TX100 containing buffers enabled elution of MmpL3$_{Msm}$ as homogenous peaks, OG, C12E8, TW20, FC12 appeared less favorable to stabilize MmpL3$_{Msm}$. However, the elution peak of the best detergents is not sufficient to compare their efficacy as the number of detergent molecules binding to membrane proteins dictates the detergent belt size around the proteins [38]. Consequently, it remains difficult to compare and state for example that CHAPSO (elution volume of 16.4 mL) is a better detergent than SD (elution volume of 15.8 mL).

Nevertheless, a clear correlation between the thermal stability of MmpL3$_{Msm}$ and its SEC elution profile could be drawn. We noticed that MmpL3$_{Msm}$ thermal denaturation was in line with the appearance of large protein aggregates on SDS-PAGE. We observed also a smeary band at around 70 kDa particularly pronounced for DM, DDM, FC12 and SD. We could not fully interpret this behaviour but we think the combined influence of heating with a certain type of detergent may trigger this migration pattern.

Four surfactants (TW20, OG, C12E8, and, TX100) failed at eluting MmpL3$_{Msm}$ as a very sharp and homogenous peak and led to poor thermal stability (Fig. 6). All presented aggregation at low temperatures, and even at 4 °C in the case of OG. FC12 is the exception as MmpL3$_{Msm}$ seems to be stable in this detergent but presents degrees of aggregation on SEC. This could be interpreted by the fact that even if MmpL3$_{Msm}$ is denatured at high temperature, FC12 is a very harsh detergent it might still keep aggregated MmpL3$_{Msm}$ as soluble forms. CHAPSO is also an exception, albeit difficult to rationalize, as SEC elution

profile with this detergent looks of high quality but is not supported by the thermal stability assay as the protein aggregates at low temperature.

We propose that peptidiscs could represent an alternative to maintain MmpL3$_{Msm}$ soluble in a detergent-free buffer. The assessment of several MmpL3$_{Msm}$::NSPr molar ratios clearly showed that the optimal result was obtained with a ratio of 1:20. In these conditions, the protein eluted on SEC slightly after DM or DDM. The delay in elution as compared with the detergents could be explained by the fact that the apparent molecular weight (94 kDa) of the protein in complex with peptidiscs is lower than with the protein surrounded by the detergent belt. In line with these findings, it was previously shown that peptidiscs can displace detergents molecules surrounding the protein and that only some lipids from the expressing host remain attached to the protein [30]. The apparent stabilization of MmpL3$_{Msm}$ into peptidiscs was further confirmed by the thermal stability assay whereby the behavior of the protein appeared similar to the best detergents, associated with a decrease in protein stability at concentrations above 50 °C. So far, MmpL3$_{Msm}$ purification was reported only in DDM, while the purification of MmpL3 from *M. tuberculosis* was also achieved using LMNG. Purification of the MmpL3 homologue from Corynebacteria was also performed using DDM [16]. From a biochemical perspective, the present work adds novelty as three new detergents, namely DM, LDAO, and SD as well as peptidisc insertion offer new options to stabilize MmpL3Msm in solution.

Although very important breakthroughs on the structural and biochemical aspects of TMM transport mechanism or inhibition arose recently, the present study appears particularly interesting for future studies on MmpL3. Enlarging the repertoire of useful detergents to purify MmpL3 may ease i) the investigation of MmpL3 activity *in vitro*; ii) the development of binding assays to determine affinity constants of MmpL3 substrates and inhibitors; and iii) future structural studies, such as MmpL3 in complex with its binding partners. The latter point is of interest since the remaining challenges to fully understand TMM transport will undoubtedly rely on the role of the MmpL3 accessory proteins [7], including TmaT [39]. Although DDM is an efficient detergent, widely used to extract membrane-associated MmpL3 accessory proteins from the source organism (i.e. TtfA [7]), one cannot exclude that the different MmpL3 membrane protein partners can be purified in sufficient amounts with this surfactant. Along the same lines, investigation of complex formation of MmpL3 with its soluble binding partners [39,40] may require detergent-free conditions. This work, expanding the currently available detergent panel used to solubilize and stabilize MmpL3Msm is paving the way for the search of optimal conditions to stabilize MmpL3 transport complexes for subsequent biochemical and structural investigations.

The highest structural resolution (2.2 Å) obtained so far for MmpL3 has been achieved by Cryo-EM using detergent-free buffer, thanks to the insertion of MmpL3 in

nanodiscs [22]. This strategy has demonstrated its potential and efficacy for solving the structure of numerous membrane proteins. Nonetheless, one limitation of nanodiscs is the size of the protein or protein complex that can be embedded into the nanoparticles and this requires also extensive work to identify the appropriate lipids for the relipidation step. In contrast, the peptidisc technology which has also been successfully used in structural investigations of membrane proteins [30,41] has a great advantage over nanodiscs to not be limited by the size of the protein. The demonstration that it is possible to incorporate $MmpL3_{Msm}$ into peptidiscs offers an alternative without size and detergent restriction to further investigate MmpL3 and its binding partners.

Declaration of competing interest

The authors declare no competing interests.

Funding

This work was funded by the National Research Agency (ANR-17-CE11-0008-01 – MyTraM to MB) and The Lundbeck Foundation, Denmark (R303-2018-2964 to HA).

CRediT authorship contribution statement

Kien Lam Ung: Conceptualization, Methodology, Formal analysis, Investigation, Writing – review & editing. Husam Alsarraf: Conceptualization, Methodology, Formal analysis, Investigation, Writing – review & editing, Funding acquisition. Laurent Kremer: Resources, Project administration, Writing – review & editing, Funding acquisition. Mickaël Blaise: Conceptualization, Methodology, Formal analysis, Investigation, Resources, Project administration, Supervision, Writing – original draft, Writing – review & editing, Funding acquisition.

Acknowledgments

We acknowledge the Paul Scherrer Institut, Villigen, Switzerland for the provision of synchrotron radiation beamtime at beamline SLS-PXIII-X06DA of the SLS and would like to thank Dr. C.Y. Huang and Dr. K. McAuley for their assistance. We thank the European Synchrotron Radiation Facility, Grenoble, France, for providing beamtime and the staff members of the MASSIF-1 beamline for assistance during data collection. We thank Dr M. Picard for the gift of the *E. coli* C43(DE3)*ΔacrB* strain.

References

[1] WHO | Global tuberculosis report 2020, WHO. (n.d.). http://www.who.int/tb/publications/global_report/en/ (accessed November 10, 2020).
[2] M.D. Johansen, J.-L. Herrmann, L. Kremer, Non-tuberculous mycobacteria and the rise of Mycobacterium abscessus, Nat. Rev. Microbiol. 18 (2020) 392–407. https://doi.org/10.1038/s41579-020-0331-1.
[3] Y.-M. Boudehen, L. Kremer, Mycobacterium abscessus, Trends Microbiol. (2021). https://doi.org/10.1016/j.tim.2021.06.006.
[4] A. Quémard, New Insights into the Mycolate-Containing Compound Biosynthesis and Transport in Mycobacteria, Trends Microbiol. 24 (2016) 725–738. https://doi.org/10.1016/j.tim.2016.04.009.
[5] A.E. Grzegorzewicz, H. Pham, V.A.K.B. Gundi, M.S. Scherman, E.J. North, T. Hess, V. Jones, V. Gruppo, S.E.M. Born, J. Korduláková, S.S. Chavadi, C. Morisseau, A.J. Lenaerts, R.E. Lee, M.R. McNeil, M. Jackson, Inhibition of mycolic acid transport across the Mycobacterium tuberculosis plasma membrane, Nat. Chem. Biol. 8 (2012) 334–341. https://doi.org/10.1038/nchembio.794.
[6] C. Dupont, A. Viljoen, F. Dubar, M. Blaise, A. Bernut, A. Pawlik, C. Bouchier, R. Brosch, Y. Guérardel, J. Lelièvre, L. Ballell, J.-L. Herrmann, C. Biot, L. Kremer, A new piperidinol derivative targeting mycolic acid transport in Mycobacterium abscessus, Mol. Microbiol. 101 (2016) 515–529. https://doi.org/10.1111/mmi.13406.
[7] A. Fay, N. Czudnochowski, J.M. Rock, J.R. Johnson, N.J. Krogan, O. Rosenberg, M.S. Glickman, Two Accessory Proteins Govern MmpL3 Mycolic Acid Transport in Mycobacteria, MBio. 10 (2019). https://doi.org/10.1128/mBio.00850-19.
[8] K.L. Ung, H.M.A.B. Alsarraf, L. Kremer, M. Blaise, The crystal structure of the mycobacterial trehalose monomycolate transport factor A, TtfA, reveals an atypical fold, Proteins Struct. Funct. Bioinforma. 88 (2020) 809–815. https://doi.org/10.1002/prot.25863.
[9] A. Bhatt, V. Molle, G.S. Besra, W.R. Jacobs, L. Kremer, The Mycobacterium tuberculosis FAS-II condensing enzymes: their role in mycolic acid biosynthesis, acid-fastness, pathogenesis and in future drug development, Mol. Microbiol. 64 (2007) 1442–1454. https://doi.org/10.1111/j.1365-2958.2007.05761.x.
[10] A. Viljoen, V. Dubois, F. Girard-Misguich, M. Blaise, J.-L. Herrmann, L. Kremer, The diverse family of MmpL transporters in mycobacteria: from regulation to antimicrobial developments, Mol. Microbiol. (2017). https://doi.org/10.1111/mmi.13675.
[11] J.P. Sethiya, M.A. Sowards, M. Jackson, E.J. North, MmpL3 Inhibition: A New Approach to Treat Nontuberculous Mycobacterial Infections, Int. J. Mol. Sci. 21 (2020). https://doi.org/10.3390/ijms21176202.
[12] K. Tahlan, R. Wilson, D.B. Kastrinsky, K. Arora, V. Nair, E. Fischer, S.W. Barnes, J.R. Walker, D. Alland, C.E. Barry, H.I. Boshoff, SQ109 targets MmpL3, a membrane transporter of trehalose monomycolate involved in mycolic acid donation to the cell wall core of Mycobacterium tuberculosis, Antimicrob. Agents Chemother. 56 (2012) 1797–1809. https://doi.org/10.1128/AAC.05708-11.

[13] M. Biava, G.C. Porretta, F. Manetti, New derivatives of BM212: A class of antimycobacterial compounds based on the pyrrole ring as a scaffold, Mini Rev Med Chem. 7 (2007) 65–78.
[14] C. Dupont, Y. Chen, Z. Xu, F. Roquet-Banères, M. Blaise, A.-K. Witt, F. Dubar, C. Biot, Y. Guérardel, F.P. Maurer, S.-S. Chng, L. Kremer, A piperidinol-containing molecule is active against Mycobacterium tuberculosis by inhibiting the mycolic acid flippase activity of MmpL3, J. Biol. Chem. 294 (2019) 17512–17523. https://doi.org/10.1074/jbc.RA119.010135.
[15] C. Raynaud, W. Daher, M.D. Johansen, F. Roquet-Banères, M. Blaise, O.K. Onajole, A.P. Kozikowski, J.-L. Herrmann, J. Dziadek, K. Gobis, L. Kremer, Active Benzimidazole Derivatives Targeting the MmpL3 Transporter in Mycobacterium abscessus, ACS Infect. Dis. 6 (2020) 324–337. https://doi.org/10.1021/acsinfecdis.9b00389.
[16] J.M. Belardinelli, A. Yazidi, L. Yang, L. Fabre, W. Li, B. Jacques, S.K. Angala, I. Rouiller, H.I. Zgurskaya, J. Sygusch, M. Jackson, Structure-Function Profile of MmpL3, the Essential Mycolic Acid Transporter from Mycobacterium tuberculosis, ACS Infect Dis. 2 (2016) 702–713. https://doi.org/10.1021/acsinfecdis.6b00095.
[17] C.-C. Su, P.A. Klenotic, J.R. Bolla, G.E. Purdy, C.V. Robinson, E.W. Yu, MmpL3 is a lipid transporter that binds trehalose monomycolate and phosphatidylethanolamine, Proc. Natl. Acad. Sci. U. S. A. 116 (2019) 11241–11246. https://doi.org/10.1073/pnas.1901346116.
[18] X. Yang, T. Hu, X. Yang, W. Xu, H. Yang, L.W. Guddat, B. Zhang, Z. Rao, Structural Basis for the Inhibition of Mycobacterial MmpL3 by NITD-349 and SPIRO, J. Mol. Biol. 432 (2020) 4426–4434. https://doi.org/10.1016/j.jmb.2020.05.019.
[19] B. Zhang, J. Li, X. Yang, L. Wu, J. Zhang, Y. Yang, Y. Zhao, L. Zhang, X. Yang, X. Yang, X. Cheng, Z. Liu, B. Jiang, H. Jiang, L.W. Guddat, H. Yang, Z. Rao, Crystal Structures of Membrane Transporter MmpL3, an Anti-TB Drug Target, Cell. 176 (2019) 636-648.e13. https://doi.org/10.1016/j.cell.2019.01.003.
[20] I. Alav, J. Kobylka, M.S. Kuth, K.M. Pos, M. Picard, J.M.A. Blair, V.N. Bavro, Structure, Assembly, and Function of Tripartite Efflux and Type 1 Secretion Systems in Gram-Negative Bacteria, Chem. Rev. (2021). https://doi.org/10.1021/acs.chemrev.1c00055.
[21] O. Adams, J.C. Deme, J.L. Parker, CRyPTIC Consortium, P.W. Fowler, S.M. Lea, S. Newstead, Cryo-EM structure and resistance landscape of M. tuberculosis MmpL3: An emergent therapeutic target, Struct. Lond. Engl. 1993. (2021) S0969-2126(21)00217–3. https://doi.org/10.1016/j.str.2021.06.013.
[22] C.-C. Su, P.A. Klenotic, M. Cui, M. Lyu, C.E. Morgan, E.W. Yu, Structures of the mycobacterial membrane protein MmpL3 reveal its mechanism of lipid transport, PLoS Biol. 19 (2021) e3001370. https://doi.org/10.1371/journal.pbio.3001370.
[23] J. de Ruyck, C. Dupont, E. Lamy, V. Le Moigne, C. Biot, Y. Guérardel, J.-L. Herrmann, M. Blaise, S. Grassin-Delyle, L. Kremer, F. Dubar, Structure-Based Design and Synthesis of Piperidinol-Containing Molecules as New Mycobacterium abscessus Inhibitors, ChemistryOpen. 9 (2020) 351–365. https://doi.org/10.1002/open.202000042.
[24] M. Korycka-Machała, A. Viljoen, J. Pawełczyk, P. Borówka, B. Dziadek, K. Gobis, A. Brzostek, M. Kawka, M. Blaise, D. Strapagiel, L. Kremer, J. Dziadek, 1H-Benzo[d]Imidazole Derivatives Affect MmpL3 in Mycobacterium tuberculosis, Antimicrob. Agents Chemother. 63 (2019). https://doi.org/10.1128/AAC.00441-19.

[25] Z. Xu, V.A. Meshcheryakov, G. Poce, S.-S. Chng, MmpL3 is the flippase for mycolic acids in mycobacteria, Proc. Natl. Acad. Sci. U. S. A. 114 (2017) 7993–7998. https://doi.org/10.1073/pnas.1700062114.
[26] M.A. Seeger, C. von Ballmoos, T. Eicher, L. Brandstätter, F. Verrey, K. Diederichs, K.M. Pos, Engineered disulfide bonds support the functional rotation mechanism of multidrug efflux pump AcrB, Nat. Struct. Mol. Biol. 15 (2008) 199–205. https://doi.org/10.1038/nsmb.1379.
[27] W. Kabsch, Integration, scaling, space-group assignment and post-refinement, Acta Crystallogr. D Biol. Crystallogr. 66 (2010) 133–144. https://doi.org/10.1107/S0907444909047374.
[28] A.J. McCoy, R.W. Grosse-Kunstleve, P.D. Adams, M.D. Winn, L.C. Storoni, R.J. Read, Phaser crystallographic software, J. Appl. Crystallogr. 40 (2007) 658–674. https://doi.org/10.1107/S0021889807021206.
[29] P.D. Adams, P.V. Afonine, G. Bunkóczi, V.B. Chen, I.W. Davis, N. Echols, J.J. Headd, L.-W. Hung, G.J. Kapral, R.W. Grosse-Kunstleve, A.J. McCoy, N.W. Moriarty, R. Oeffner, R.J. Read, D.C. Richardson, J.S. Richardson, T.C. Terwilliger, P.H. Zwart, PHENIX: a comprehensive Python-based system for macromolecular structure solution, Acta Crystallogr. D Biol. Crystallogr. 66 (2010) 213–221. https://doi.org/10.1107/S0907444909052925.
[30] M.L. Carlson, J.W. Young, Z. Zhao, L. Fabre, D. Jun, J. Li, J. Li, H.S. Dhupar, I. Wason, A.T. Mills, J.T. Beatty, J.S. Klassen, I. Rouiller, F. Duong, The Peptidisc, a simple method for stabilizing membrane proteins in detergent-free solution, ELife. 7 (2018). https://doi.org/10.7554/eLife.34085.
[31] Z.E.R. Newby, J.D. O'Connell, F. Gruswitz, F.A. Hays, W.E.C. Harries, I.M. Harwood, J.D. Ho, J.K. Lee, D.F. Savage, L.J.W. Miercke, R.M. Stroud, A general protocol for the crystallization of membrane proteins for X-ray structural investigation, Nat. Protoc. 4 (2009) 619–637. https://doi.org/10.1038/nprot.2009.27.
[32] A. Stetsenko, A. Guskov, An Overview of the Top Ten Detergents Used for Membrane Protein Crystallization, Crystals. 7 (2017) 197. https://doi.org/10.3390/cryst7070197.
[33] J.-L. Popot, Amphipols, nanodiscs, and fluorinated surfactants: three nonconventional approaches to studying membrane proteins in aqueous solutions, Annu. Rev. Biochem. 79 (2010) 737–775. https://doi.org/10.1146/annurev.biochem.052208.114057.
[34] S.C. Lee, T.J. Knowles, V.L.G. Postis, M. Jamshad, R.A. Parslow, Y. Lin, A. Goldman, P. Sridhar, M. Overduin, S.P. Muench, T.R. Dafforn, A method for detergent-free isolation of membrane proteins in their local lipid environment, Nat. Protoc. 11 (2016) 1149–1162. https://doi.org/10.1038/nprot.2016.070.
[35] I.G. Denisov, S.G. Sligar, Nanodiscs in Membrane Biochemistry and Biophysics, Chem. Rev. 117 (2017) 4669–4713. https://doi.org/10.1021/acs.chemrev.6b00690.
[36] J. Frauenfeld, R. Löving, J.-P. Armache, A.F.-P. Sonnen, F. Guettou, P. Moberg, L. Zhu, C. Jegerschöld, A. Flayhan, J.A.G. Briggs, H. Garoff, C. Löw, Y. Cheng, P. Nordlund, A saposin-lipoprotein nanoparticle system for membrane proteins, Nat. Methods. 13 (2016) 345–351. https://doi.org/10.1038/nmeth.3801.

[37] A. Viljoen, V. Dubois, F. Girard-Misguich, M. Blaise, J.-L. Herrmann, L. Kremer, The diverse family of MmpL transporters in mycobacteria: from regulation to antimicrobial developments, Mol. Microbiol. 104 (2017) 889–904. https://doi.org/10.1111/mmi.13675.
[38] V. Chaptal, F. Delolme, A. Kilburg, S. Magnard, C. Montigny, M. Picard, C. Prier, L. Monticelli, O. Bornert, M. Agez, S. Ravaud, C. Orelle, R. Wagner, A. Jawhari, I. Broutin, E. Pebay-Peyroula, J.-M. Jault, H.R. Kaback, M. le Maire, P. Falson, Quantification of Detergents Complexed with Membrane Proteins, Sci. Rep. 7 (2017) 41751. https://doi.org/10.1038/srep41751.
[39] J.M. Belardinelli, C.M. Stevens, W. Li, Y.Z. Tan, V. Jones, F. Mancia, H.I. Zgurskaya, M. Jackson, The MmpL3 interactome reveals a complex crosstalk between cell envelope biosynthesis and cell elongation and division in mycobacteria, Sci. Rep. 9 (2019) 10728. https://doi.org/10.1038/s41598-019-47159-8.
[40] G.C. Melly, H. Stokas, J.L. Dunaj, F.F. Hsu, M. Rajavel, C.-C. Su, E.W. Yu, G.E. Purdy, Structural and functional evidence that lipoprotein LpqN supports cell envelope biogenesis in Mycobacterium tuberculosis, J. Biol. Chem. 294 (2019) 15711–15723. https://doi.org/10.1074/jbc.RA119.008781.
[41] G. Angiulli, H.S. Dhupar, H. Suzuki, I.S. Wason, F. Duong Van Hoa, T. Walz, New approach for membrane protein reconstitution into peptidiscs and basis for their adaptability to different proteins, ELife. 9 (2020) e53530. https://doi.org/10.7554/eLife.53530.